Journal of Aeronautics & Aerospace Engineering

Yeh and Yeh, J Aeronaut Aerospace Eng 2014, 3:1
DOI: 10.4172/2168-9792.1000129

Research Article | Open Access

A Dimensionless Analysis of Stress Distribution for Hydrostatic Tension in an Orthotropic Plate

Hsien-Liang Yeh[1]* and Hsien-Yang Yeh[2]

[1]*Department of Civil and Ecological Engineering, I-Shou University, Kaohsiung City 84001, Taiwan*
[2]*Department of Mechanical Engineering, California State University, Long Beach, CA, USA*

Abstract

The effect of lamina material properties on the stress distribution of the orthotropic composite plate containing a circular cutout under hydrostatic tension is investigated. Based on the generalized Hooke's law, the generalized plane stress condition and the complex variable method, a dimensionless analysis is used to evaluate the influence of various elastic moduli E_1, E_2, G_{12} and v_{12} on the stress distribution along the boundary of the cutout in the composite plate under hydrostatic tension. The results obtained from this dimensionless analysis provide a set of general design guidelines for structural laminates with high precision requirements in the engineering applications.

Keywords: Hydrostatic tension; Stress distribution; Orthotropic plate; Complex variable; Composite materials

Introduction

Composite materials consist of various fibrous reinforcements coupled with a compatible matrix to achieve superior structural performance. The selection of composite materials for specific applications is generally determined by the physical and mechanical properties of the materials, evaluated for both function and fabrication [1]. Knowledge of stress distributions in anisotropic materials is very important for proper use of these new high-performance materials in structural applications [2].

Kuwamura [3] analyzed the stresses around the circular cutout by means of Ikeda's formula in consideration of orthotropic elasticity of the woods, which revealed that the stresses distribution around the circular hole is nearly equal to that of an isotropic plate. Selivanov [4] studied the time variation in the stresses around an elliptic hole in a composite plate. Kumar et al. [5] presented an approximate solution in the form of a polynomial for the normal stress distribution adjacent to a class of optimum holes in symmetrically laminated infinite composite plates under uniaxial loading. Giare and Shabahang [6] used a finite element analysis to calculate the stress distribution around a hole in a finite isotropic plate reinforced by composite material. Tsai et al. [7] developed a novel procedure for predicting the notched strengths of composite plates each with a center hole. And the stress distribution of a composite plate with a center hole is obtained by a finite element analysis.

In this paper, the effect of lamina material properties on the stress distribution of the orthotropic composite plate containing a circular cutout under hydrostatic tension is investigated. Based on the generalized Hooke's law, the generalized plane stress in an orthotropic composite plate and the complex variable method, a dimensionless analysis is used to evaluate the influence of various elastic moduli E_1, E_2, G_{12} and v_{12} on the stress distribution along the boundary of the circular cutout in the composite plate under hydrostatic tension.

Tangential Stresses on the Boundary of the Circular Opening

The stress-strain distribution of an infinite anisotropic plate containing a through-the-thickness cutout has been derived using a complex variable method [8-10]. For an orthotropic plate subjected to equal tensile stress p in two principal directions which are applied at a considerable distance from the circular opening as shown in Figure 1 (and this is equivalent to hydrostatic tension in plane xy). The normal stress component σ_θ for an element tangential to the opening is [9]

$$\sigma_\theta = p\,\frac{E_\theta}{E_1}\,[-k + k\,(k+n)\cos^2\theta + (1+n)\sin^2\theta] \tag{1}$$

where

$$k = \sqrt{\frac{E_1}{E_2}} \tag{2}$$

$$n = \sqrt{\frac{E_1}{G_{12}} - 2\,\nu_{12} + 2\sqrt{\frac{E_1}{E_2}}} \tag{3}$$

The θ is the polar angle measured from the x-axis; E_θ is the Young's modulus in tension (compression) along the direction tangent to the opening contour, which is related to elastic constants in the principal directions by the formula

$$\frac{1}{E_\theta} = \frac{\sin^4\theta}{E_1} + \left(\frac{1}{G_{12}} - \frac{2\,\nu_{12}}{E_1}\right)\sin^2\theta\cos^2\theta + \frac{\cos^4\theta}{E_2} \tag{4}$$

For an isotropic plate [9]

$$\sigma_\theta = 2p \tag{5}$$

A Dimensionless Analysis Model for Evaluation of the Normal Stress σ_θ

Consider the orthotropic plate containing a circular hole under hydrostatic tension. For a dimensionless analysis, the three lamina

***Corresponding author:** Dr. Hsien-Liang Yeh, Department of Civil and Ecological Engineering, I-Shou University, Kaohsiung City 84001, Taiwan, Tel:886-7-6577711ext.3315; E-mail: hlyeh@isu.edu.tw

Received May 21, 2014; **Accepted** July 05, 2014; **Published** July 11, 2014

Citation: Yeh HL, Yeh HY (2014) A Dimensionless Analysis of Stress Distribution for Hydrostatic Tension in an Orthotropic Plate. J Aeronaut Aerospace Eng 3: 129. doi:10.4172/2168-9792.1000129

Citation: Yeh HL, Yeh HY (2014) A Dimensionless Analysis of Stress Distribution for Hydrostatic Tension in an Orthotropic Plate. J Aeronaut Aerospace Eng 3: 129. doi:10.4172/2168-9792.1000129

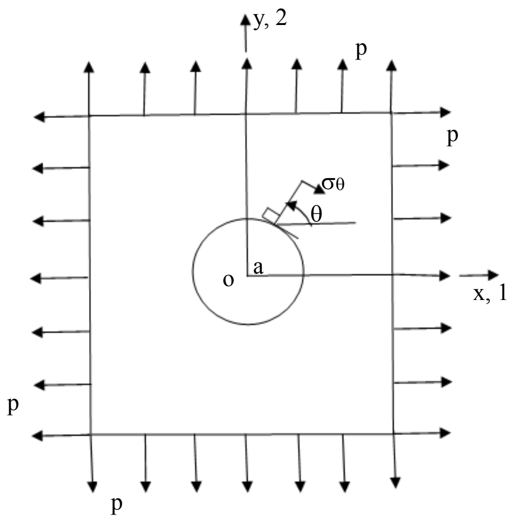

Figure 1: An orthotropic plate containing a circular hole under hydrostatictension with principal material axes 1-2 and x-y axes.

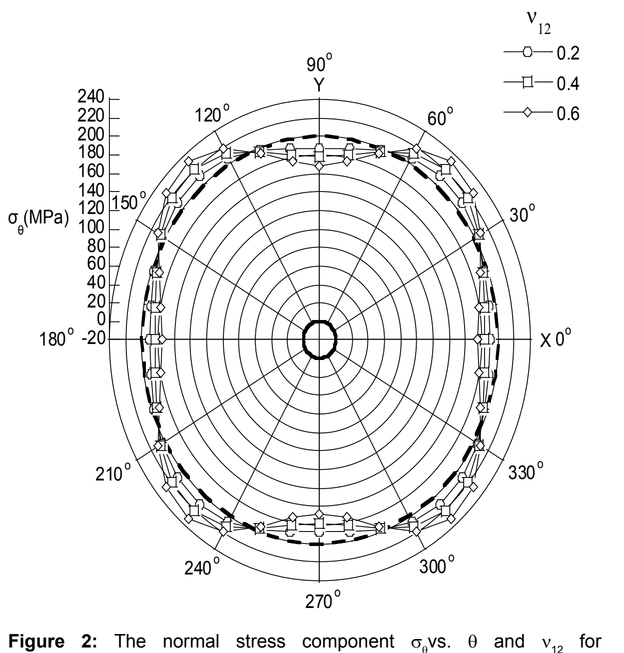

Figure 2: The normal stress component $\sigma_\theta$vs. θ and ν_{12} for p=100MPa,E_1=204GPa, E_2/E_1=0.6, and G_{12}/E_1=0.4.

material constants E_1, E_2 and G_{12} are represented by two dimensionless ratios E_2/E_1 and G_{12}/E_1. Totally, the lamina material has three parameters E_2/E_1, G_{12}/E_1 and ν_{12}. For an unidirectional lamina with different values of E_2/E_1, G_{12}/E_1 and ν_{12}, the normal stress component σ_θ of the orthotropic plate under the hydrostatic tension will be varied and provided different values.

Various cases of different combinations of the three material parameters are considered in this study. In general case, the ranges of E_2/E_1 and G_{12}/E_1 are between zero and one, the ranges of ν_{12} are between 0 and 0.6. For a lamina with given material properties E_2/E_1, G_{12}/E_1 and ν_{12}, the normal stress component σ_θ of the orthotropic plate under the hydrostatic tension can be evaluated.

Results and Discussion

In the (Figures 2-4), the bold solid line represents the circular hole and the bold dotted line shows the stress distribution σ_θ in an isotropic plate subjected to identical load as in an orthotropic plate. The stress distribution for an orthotropic plate is symmetrical with respect to the opening center. Thus, the variation of the stress distribution $_\theta$ is considered only in the range of 0° ≤ θ ≤ 180° for an orthotropic plate. In an isotropic plate given p=100 MPa, then calculated from Equation (5), the constant stress σ_θ is 200 MPa. Therefore, the stress concentration factor in an isotropic plate is S_c=2.0. It is well known that the stress concentration factor for a circular cutout in the isotropic thin plate under uni-axial tensile load is "three". However, in this study, tensile stresses in two perpendicular directions equal to p are applied in the thin plate with a circular cutout, therefore, through the linear superposition, it is found the stress concentration factor for this isotropic plate is S_c=2.0.

In Table 1 given p=100 MPa, E_1=204 GPa, E_2/E_1=0.6 and G_{12}/E_1=0.4, the variation of the stress σ_θ with respect to the polar angle θ and ν_{12} is the following:

With ν_{12}=0.2, 0.4, and 0.6, the minimum corresponding stresses σ_θ are 187.28 MPa, 177.83 MPa, and 167.93 MPa at θ=90° respectively, and the maximum stresses σ_θ are 211.62 MPa, 221.17 MPa, and 232.14 MPa at θ=50° as well as θ=130° respectively. Also, the stress concentration factors are S_c=2.12, 2.21, and 2.32 respectively, for orthotropic case.

Table 1 shows that within the ranges of the polar angle 0° ≤ θ ≤ 20°, 70° θ ≤ 110°, and 160° ≤ θ ≤ 180°, the stress σ_θ decreases along with the increased values of ν_{12}. But, within the ranges of the polar angle 30° ≤ θ ≤ 60° and 120° ≤ θ ≤ 150°, the stress $_\theta$ increases along with the increased values of $\nu_{12.}$ A summary of Table 1 is shown in Figure 2.

In Table 2 given p=100 MPa, E_1=204 GPa, E_2/E_1=0.6 and ν_{12}=0.4, the variation of the stress σ_θ with respect to the polar angle θ and G_{12}/E_1 is following:

With G_{12}/E_1=0.2, 0.4, 0.6, 0.8 and 1.0, the minimum corresponding

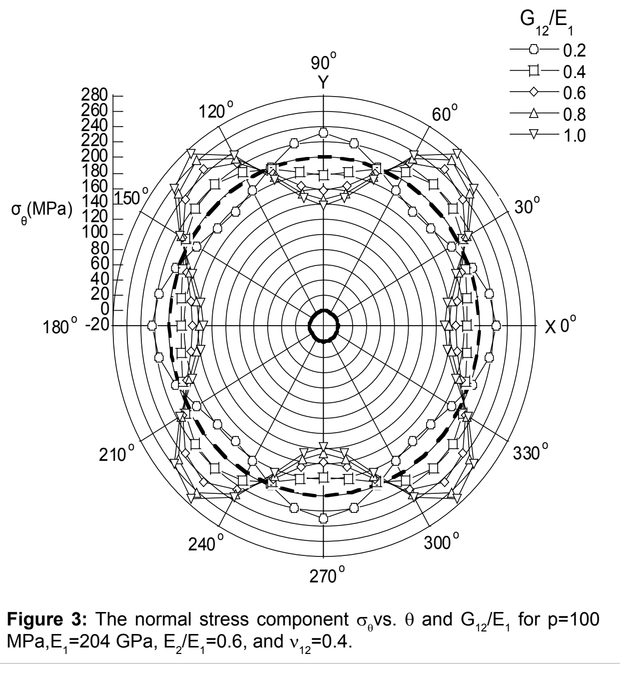

Figure 3: The normal stress component $\sigma_\theta$vs. θ and G_{12}/E_1 for p=100 MPa,E_1=204 GPa, E_2/E_1=0.6, and ν_{12}=0.4.

Citation: Yeh HL, Yeh HY (2014) A Dimensionless Analysis of Stress Distribution for Hydrostatic Tension in an Orthotropic Plate. J Aeronaut Aerospace Eng 3: 129. doi:10.4172/2168-9792.1000129

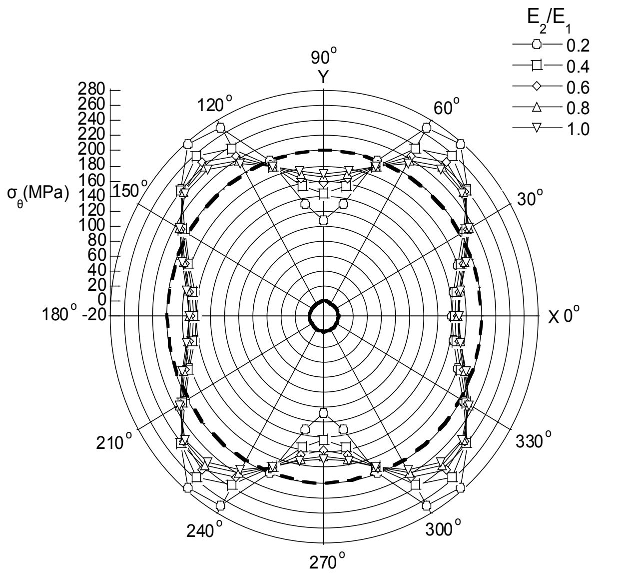

Figure 4: The normal stress component σ_θ vs. θ and E_2/E_1 for p=100 MPa, E_1=204 GPa, G_{12}/E_1=0.6, and ν_{12}=0.4.

	σ_θ(MPa)		
θ \ ν_{12}	**0.2**	**0.4**	**0.6**
0°	190.1468	182.8274	175.1573
10°	192.0270	185.9280	179.3790
20°	197.2014	194.6964	191.6553
30°	204.1280	207.0080	209.7919
40°	210.0384	218.0841	227.1022
50°	211.6244	221.1711	232.1421
60°	207.1710	212.6519	218.5025
70°	198.5809	196.9797	194.7377
80°	190.5158	183.1520	175.1465
90°	187.2796	177.8302	167.9282
100°	190.5158	183.1520	175.1465
110°	198.5809	196.9797	194.7377
120°	207.1710	212.6519	218.5025
130°	211.6244	221.1711	232.1421
140°	210.0384	218.0841	227.1022
150°	204.1280	207.0080	209.7919
160°	197.2014	194.6964	191.6553
170°	192.0270	185.9280	179.3790
180°	190.1468	182.8274	175.1573

Table 1: The normal stress component σ_θ vs. θ and ν_{12} for p=100 MPa, E_1=204 GPa, E_2/E_1=0.6, and G_{12}/E_1=0.4.

stresses σ_θ are 176.16 MPa at θ=50° as well as =130°, and other minimum corresponding stresses σ_θ are 177.83 MPa, 156.61 MPa, 145.03 MPa and 137.69 MPa at θ=90° respectively, and the maximum stresses σ_θ are 231.32 MPa at θ=90°, 221.17 MPa, 246.09 MPa, 262.21 MPa and 273.54 MPa at θ=50° as well as θ=130° respectively. Also, the stress concentration factors are S_c=2.31, 2.21, 2.46, 2.62, and 2.73 respectively, for orthotropic case.

Table 2 shows that within the ranges of the polar angle 0° ≤ θ ≤ 20°, 70° ≤ θ ≤ 110° and 160° ≤ θ180° the stress σ decreases along with the increased values of G_{12}/E_1. But, within the ranges of the polar angle 30° ≤ θ ≤ 60° and 120° ≤ θ 150°, the stress σ_θ increases along with the increased values of G_{12}/E_1. A summary of Table 2 is shown in Figure 3.

	σ_θ(MPa)				
θ \ G_{12}/E_1	**0.2**	**0.4**	**0.6**	**0.8**	**1.0**
0°	224.2627	182.8274	166.3872	157.4178	151.7376
10°	218.4431	185.9280	171.6972	163.6331	158.4209
20°	204.4044	194.6964	187.6255	182.8601	179.4900
30°	189.1800	207.0080	212.5897	214.8970	215.9955
40°	178.6255	218.0841	238.2099	250.5184	258.8396
50°	176.1625	221.1711	246.0954	262.2070	273.5433
60°	183.5657	212.6519	225.2655	232.1585	236.4414
70°	200.5763	196.9797	191.3849	186.9838	183.6381
80°	221.2496	183.1520	165.6352	155.5200	148.9160
90°	231.3231	177.8302	156.6061	145.0266	137.6935
100°	221.2496	183.1520	165.6352	155.5200	148.9160
110°	200.5763	196.9797	191.3849	186.9838	183.6381
120°	183.5657	212.6519	225.2655	232.1585	236.4414
130°	176.1625	221.1711	246.0954	262.2070	273.5433
140°	178.6255	218.0841	238.2099	250.5184	258.8396
150°	189.1800	207.0080	212.5897	214.8970	215.9955
160°	204.4044	194.6964	187.6255	182.8601	179.4900
170°	218.4431	185.9280	171.6972	163.6331	158.4209
180°	224.2627	182.8274	166.3872	157.4178	151.7376

Table 2: The normal stress component σ_θ vs. θ and G_{12}/E_1 for p=100 MPa, E_1=204 GPa, E_2/E_1=0.6, and ν_{12}=0.4.

	σ_θ(MPa)				
θ \ E_2/E_1	**0.2**	**0.4**	**0.6**	**0.8**	**1.0**
0°	158.6111	163.7024	166.3872	168.1069	169.3123
10°	163.3198	168.7368	171.6972	173.6703	175.1163
20°	180.2301	184.1946	187.6255	189.9839	191.7611
30°	204.6600	210.0193	212.5897	214.0722	214.9998
40°	242.4456	240.8558	238.2099	235.6879	233.4666
50°	277.4915	257.6026	246.0954	238.6573	233.4666
60°	268.7737	237.4698	225.2655	218.8828	214.9998
70°	200.1263	192.3720	191.3849	191.4572	191.7611
80°	132.0207	155.5936	165.6352	171.3639	175.1163
90°	107.4517	142.6084	156.6061	164.3424	169.3123
100°	132.0207	155.5936	165.6352	171.3639	175.1163
110°	200.1263	192.3720	191.3849	191.4572	191.7611
120°	268.7737	237.4698	225.2655	218.8828	214.9998
130°	277.4915	257.6026	246.0954	238.6573	233.4666
140°	242.4456	240.8558	238.2099	235.6879	233.4666
150°	204.6600	210.0193	212.5897	214.0722	214.9998
160°	180.2301	184.1946	187.6255	189.9839	191.7611
170°	163.3198	168.7368	171.6972	173.6703	175.1163
180°	158.6111	163.7024	166.3872	168.1069	169.3123

Table 3: The normal stress component σ_θ vs. θ and E_2/E_1 for p=100 MPa, E_1=204 GPa, G_{12}/E_1=0.6, and ν_{12}=0.4.

In Table 3 given p=100 MPa, E_1=204 GPa, G_{12}/E_1=0.6 and ν_{12}=0.4, the variation of the stress σ_θ with respect to the polar angle θ and E_2/E_1 is following:

With E_2/E_1=0.2, 0.4, 0.6, 0.8 and 1.0, the minimum corresponding stresses σ_θ are 107.45 MPa, 142.61 MPa, 156.61 MPa 164.34 MPa, and 169.31 MPa at θ=90° respectively, and the maximum stresses σ are 277.49 MPa, 257.60 MPa, 246.09 MPa, 238.66 MPa and 233.47 MPa at θ=50° respectively. Moreover, for E_2/E_1=1.0, the minimum stress σ occurred at θ=0° as well as θ=180° and the maximum stress σ_θ occurred at θ=40°, θ=130° and θ=140° as well. Also, the stress concentration factors are S_c=2.77, 2.58, 2.46, 2.39, and 2.33 respectively, for orthotropic case.

Table 3 shows that within the ranges of the polar angle 0° ≤ θ ≤ 30°, 80° ≤ θ 100° and 150° ≤ θ ≤ 180°, the stress σ_θ increases along with the increased values of E_2/E_1 respectively. But, in the ranges of the polar angle 40° ≤ θ ≤ 60° and 120° ≤ θ ≤ 140°, the stress σ_θ decreases along with the increased values of E_2/E_1. As for the polar angles θ=70° as well as =110°, with the values of 0.2 ≤ E_2/E_1 ≤ 0.6, the stress σ_θ decreases along with the increased values of E_2/E_1, but for the values of 0.6 ≤ E_2/E_1 ≤ 1.0, the stress σ_θ increases along with the increased values of E_2/E_1. A summary of Table 3 is shown in Figure 4.

Conclusions

The effect of lamina material properties on the stress distribution of the orthotropic composite plate containing a circular cutout under hydrostatic tension is presented.

First of all, given fixed material parameters for E_1=204 GPa, E_2/E_1=0.6, and G_{12}/E_1=0.4 Table 1 indicates that for the values of 0.2 ≤ ν_{12} ≤ 0.6, within the ranges of the polar angle 0°≤ θ ≤ 50° and 90° ≤ θ ≤ 130°, the stress σ increases with respect to the increased values of the polar angle θ, but within the ranges of the polar angle 50° ≤ θ ≤ 90° and 130° ≤ θ ≤ 180 the stress σ_θ decreases with the increased values of the polar angle θ.

Second, given fixed material parameters for E_1=204 GPa, E_2/E_1=0.6, and ν_{12}=0.4 Table 2 indicates that for the value of G_{12}/E_1=0.2, within the ranges of the polar angle 0° ≤ θ ≤ 50° and 90° ≤ θ ≤ 130°, the stress σ_θ decreases with respect to the increased values of the polar angle θ, but within the ranges of the polar angle 50° ≤ θ ≤ 90° and 130° ≤ θ 180° the stress σ_θ increases along with the increased values of the polar angle θ.

As for the values of 0.4 ≤ G_{12}/E_1 ≤ 1.0, within the ranges of the polar angle 0° ≤ θ 50° and 90° ≤ θ ≤ 130°, the stress σ_θ increases with the increased values of polar angle θ, but within the ranges of the polar angle 50° ≤ θ ≤ 90° and 130° ≤ θ 180° the stress σ_θ decreases with respect to the increased values of the polar angle θ.

Third, given fixed material parameters for E_1=204 GPa, G_{12}/E_1=0.6, and ν_{12}=0.4 Table 3 indicates that for the values of 0.2 ≤ E_2/E_1 ≤ 1.0, within the ranges of the polar angle 0° ≤ θ ≤ 50 and 90° ≤ θ ≤ 130° the stress σ_θ increases with respect to the increased values of the polar angle θ, but within the ranges of the polar angle 50° ≤ θ ≤ 90° and 130° ≤ θ ≤ 180 the stress σ_θ decreases along with the increased values of the polar angle θ.

Fourth, it is well known that for fiber reinforced composite laminated plates, the Poisson's ratio can be negative values. However, this case is not discussed/analyzed in the present study; such investigation will be included in the future research works.

The results obtained from this dimensionless analysis provide a set of general design guidelines for structural laminates with high precision requirements in the engineering applications.

References

1. Niu, Michael CY (1992) Composite Airframe Structures. Conmilit Press Ltd, USA.
2. Sadd MH (2009) Elasticity, 2 edn. Elsevier Inc., USA.
3. Kuwamura H (2010) Splitting of Wood by Pressure in a Circular Hole: Study on Steel-Framed Timber Structures part 5.Journal of Structural and Construction Engineering, 75: 175-184.
4. Selivanov MF (2010) Influence of the Viscoelastic Properties of a Composite on the Stress Distribution around an Elliptic Hole in a Plate.International Applied Mechanics, 46: 799-805.
5. Kumar RR, Rao GV, Suresh KS (1994) Normal Stress Distribution adjacent to Optimum Holes in Composite Plates.Composite Structures, 29: 393-398.
6. Giare GS, Shabahang R (1989) Reduction of Stress Concentration around the Hole in an Isotropic Plate Using Composite Materials.Engineering Fracture Mechanics 32: 757-766.
7. Tsai KH, Hwan CL, Lin MJ, Huang YS (2012) Finite element based point stress criterion for predicting the notched strengths of composite plates.Journal of Mechanics, 28: 401-406.
8. Sih GC, Paris PC, Irwin GR (1965) On Crack in Rectilinearly Anisotropic Bodies. International Journal of Fracture, 1: 189-203.
9. Lekhnitskii SG (1968). Anisotropic Plates. USA.
10. Tan SC (1994) Stress Concentrations in Laminated Composites. USA.